Energy Systems (2019) 10:1043–1070
https://doi.org/10.1007/s12667-018-0298-4

ORIGINAL PAPER

Modeling and performance study of a parabolic trough solar power plant using molten salt storage tank in Egypt: effects of plant site location

M. H. Mohamed[1,2] · A. Z. El-Sayed[3] · K. F. Megalla[1] · H. F. Elattar[4]

Received: 15 January 2018 / Accepted: 18 July 2018 / Published online: 30 July 2018

Abstract

Modeling and performance study of large parabolic trough solar power plant using molten slat storage tank is conducted and presented for three different locations in Egypt (Aswan, Al-Arish and Hurghada) using 16 h storage system. The simulation algorithm and solar modeling have been created and simulated by *MATLAB/SIMULINK* program. A comparison between studied cities is introduced to select the best location for constructing the solar plant based on selection criteria; hot header outlet temperature, volume (hot and cold) variations during charging and discharging, and cycle power efficiency. A full design of the thermal power plant with the storage tanks is also conducted using a molten salt (60% $NaNO_3$ and 40% KNO_3). Moreover, hourly electricity plant output to obtain the influence of the thermal storage tank on the plant performance was calculated and presented. The results indicated that Aswan city is the optimum location to construct a 500 MW solar power plant under the Egyptian climate. A comparison for current model validation between simulated results and the actual results of existing plant (Archimede) was fulfilled and good agreement was obtained by maximum error 5%.

Keywords Modeling and simulation · Solar power plant · Parabolic trough · Storage tank · Molten salt

✉ M. H. Mohamed
moh75202@yahoo.de; mhmohamed@uqu.edu.sa

1 Renewable Energy Laboratory, Mechanical Power Engineering Department, Faculty of Engineering-Mattaria, Helwan University, Cairo 11718, Egypt

2 Mechanical Engineering Department, College of Engineering and Islamic Architecture, Umm Al-Qura University, P.O. 5555, Makkah, Kingdom of Saudi Arabia

3 High Institute of Engineering, Elshorouk Academy, Cairo, Egypt

4 Department of Mechanical Engineering, Benha Faculty of Engineering, Benha University, Benha, Qalyubia 13511, Egypt

List of symbols

DNI	Direct normal irradiation (W/m^2)
z	Zenith angle (°)
h	Hour angle (°)
n	Number of day (–)
IAM	Incidence angle modifier (angle)
RS	Row space (m)
W	Collector aperture width (m)
f	Focal length of collector (m)
SCA	Solar collector assemble (–)
Re	Reynolds number (dimensionless)
NU	Nusselt number (dimensionless)
ΔP	Total pressure drop per unit length (Pa/m)
D_{tank}	Storage tank diameter (m)
q_{loss}	Heat loss (kj)
SM	Solar multiple (–)
HCE	Heat collection element (–)
h_{tank}	Tank height (dimensionless)
T	Temperature (K)

Greek symbols

δ	Declination angle (°)
θ	Incident angle (°)
β	$= \frac{360}{365}(n-1)$ (°)
μ	Dynamic viscosity (N s/m^2)
ν	Kinematic viscosity (m^2/s)
ρ	Density (kg/m^3)

Abbreviations

CSP	Concentrated solar power
CSPP	Concentrated solar power plant
DNI	Direct normal irradiation
HTF	Heat transfer fluid
HEX	Heat exchanger
IAPWS IF-97	International Association for Properties of Water and Steam Industrial Formation 1997
LCoE	Levelized cost of energy
TES	Thermal energy storage
SCA	Solar collector assemble
SEGS	Solar energy generation system
SM	Solar multiple

1 Introduction

Energy crisis in any place in the worldwide is the major problem that faces the renovation and development of the countries. This energy crisis is appeared and grown due to the price rising of the fossil fuel in last decades and combustion impact on the environmental. Recently, the world is focusing in the renewable energy as reliable solution for both energy and pollution issues. Solar energy is one source of the most promising renewable energies which is abundant, wide range availability and low grad technology. Concentrating solar energy has been commercialized as a renewable energy generation technology and the most important advantage of these techniques is the possibility of being coupled to thermal energy storage systems that allows energy consumption to meet the required electricity demand.

In Egypt, energy plays an important role in the economic growth. Accordingly, Cairo Demographic Centre is expected that Egypt's population is reached to 110 million by 2031 and 128 million by 2051; this fast population growth is overstraining the restricted country energy resources, Comsan [1]. Egypt location is favorable for utilizing solar energy, where it belongs to the global sun-belt. Egypt's solar atlas was issued in 1991 and it was indicated that Egypt has 2900–3200 h (annual sunshine) with 2000–3200 kWh/m^2 (annual direct normal energy density) and solar-thermal electrical energy generation of 73.6 Peta Watt hour (PWh). Egypt in 1910 was the first country in solar energy utilization, where American engineer Frank Shuman built a solar power plant (industrial scale) at Maadi district in Cairo city using solar parabolic collectors. The generated electrical power was used to drive a set of large water pumps which used in irrigation processes.

Distribution of solar energy irradiance over Egypt according to Egyptian atlas introduces that the intensity of solar radiation increases from north to south with relatively daily unchanged profiles with small variations in resources. These conditions are helped to support of 9–11 h of sunlight per day, with few yearly cloudy days number. Therefore, Egypt has very interesting solar resources for different applications of solar energy. Where, the solar radiation has been estimated to be 74 billion MWh per year.

Engineers developed solar plants with different designs, which effectively utilized the solar energy as energy source. A thermal model of SEGS (solar electric generating systems at rated 30 MW_{el}) solar field and power cycle using EASY simulation software is introduced by Lippke [2]. The simulated model was used to predict the system characteristics during part-load situations. The model had been validated with the experimental hourly measurements of the plant for both a clear summer and winter days. Some researchers from Sandia National Laboratories and KJC [3] introduced another SEGS VI model using TRNSYS. Blair et al. [4] studied the enhancement of parabolic trough plant modeling by TRNSYS. In addition, they investigated the transient ability of the plant over small times (i.e. plant start-up and shut-down). Intended for a research focused on solar field control, Stuetzle [5] gave a thermodynamic empirical solar power plant model to assess the advances of linearized automatic control of heat transfer fluid (HTF) mass flow rate over the solar field to keep a constant outlet fluid temperature. The study showed that automatic control of the field has not significant improvement on the power output of the plant. Forristall [6] studied the thermal gains and losses over the heat collection element by thermodynamic analysis.

Moreover, He validated his model with many collectors sets performance data to study influencing parameters (absorber tube materials, annulus gases, surface coatings, and glass envelope diameters) on HCE performance. Patnode [7] developed thermodynamic model for solar field by using TRNSYS program, where the Rankine power cycle was modeled with a simultaneous equation solving software. The performance of the power cycle in steady state mode was retreated in terms of the heat transfer, fluid temperature, mass flow rate and condensing pressure. Moreover, steam condenser and cooling tower TRANSYS models were also included in the simulation. Isabel et al. [8] introduced a model for studying the performance of solar power plants using parabolic trough and thermal storage system. The aim of this model is supporting the estimation of the power output of these plants throughout the various phases of their planning, design, construction and operation.

In energy production, industrial process, desalination, air-conditioning, refrigeration, chemistry production, and irrigation, the parabolic trough solar collector is one of the most promising technologies as reported by Fernandez et al. [9] and Hepbasli and Alsuhaibani [10]. By using direct normal irradiation (DNI), the solar field produces thermal energy, and transfers this energy into a steam power plant. Generally, the solar field design depends on plant size, the temperature, the piping system pressure losses and the specific ambient conditions. Parabolic trough fields can be constructed in any direction, but erected in a north–south direction leads to the highest possible energy yield over the year.

Recently, the available oils are restricted to operate lower $\approx$ 400 °C, however, high HTF operating temperatures are needed to attain higher efficiency for Rankine cycle. The desired pressure for operating at higher temperatures is too expensive. Accordingly, fossil fuels are still needed for further superheating the generated steam by the oils to attain the desired higher temperatures in the turbine, Zhen and Suresh [11]. In the Solar systems, many existing molten salt formulations, mixtures of nitrates or nitrites have been used. The binary salt mixture is 60 wt% $NaNO_3$–40 wt% KNO_3, which has higher thermal stability (600 °C) and lower cost as well as higher melting point (220 °C). Moreover, ternary (53 wt% KNO_3–7 wt% $NaNO_3$–40 wt% $NaNO_2$) has been used many decades ago in the heat-treating industry. This salt has the lower melting point (120 °C) and it is thermal stable up to 454 °C. But, a disadvantage of these molten salts as HTF is relatively higher melting temperature which limits their usage in concentrated solar power (CSP) applications, Bradshaw [12]. The main shortcoming of molten salts is the high melting temperature; therefore, it is necessary to install an electric heater to keep the salts temperature above its melting points to avoid equipment sever harm, Zhen and Suresh [13]. The thermal properties of these molten salts such as density, viscosity, thermal conductivity and specific heat are function in the temperature Roberta et al. [14].

The thermal storages recently play an important role for the economic success of solar power plants. In parabolic trough solar plants sensible heat storages which operates with temperatures between 290 and 550 °C, are used recently. The storage influences with the operating conditions of the solar thermal plant. A change in the available solar radiation leads to change the electrical output without suitable storage. This not only leads to the plant having a supply reduction security, but also reduce lifetime of the steam turbine itself. Repeated changes to the load of the turbine lead

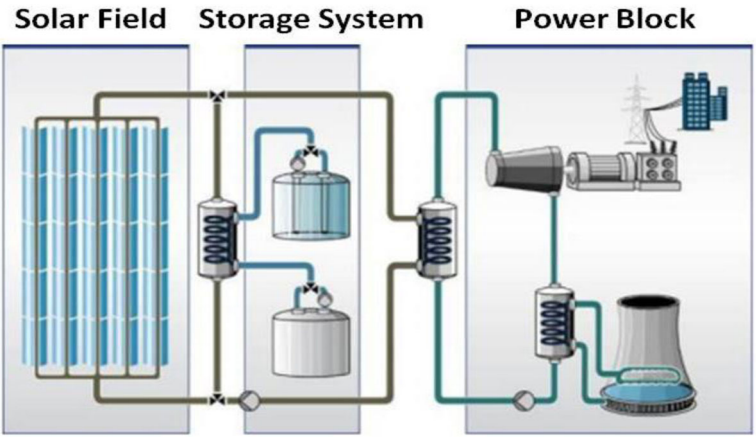

Fig. 1 Parabolic troughs concentrators, CSPP with thermal storage

to more thermal stresses and reducing the lifetime of the turbine. Therefore, larger storage techniques are able to support load shift to non-day times. By combination with an over dimension of the solar field, the operational hours can be presented significantly. Therefore, the operation time of around 2000 h per year can be extended to 4000 h per year; this is by doubling the solar field and storing the produced energy during the day. The solar multiple can rise up to 8000 operating hours per year. This allows solar multiple (SM) to operate as base load plants. SM is used as an indicator for the oversized solar field is, Daniel [15]. Figure 1 displays one possible arrangement of a concentrated solar power plant (CSPP) with thermal storage system.

1.1 Work objectives

This work is one of our targets in renewable energy in our group which dealing all renewable energies researches such solar energy [16, 17], wind energy [18–24], wave energy [25–27], and energy systems developments [28–33]. According to the authors' review, all the research papers discussed in the present review were tried to understand the performance of the CSP with thermal storage as well as cost analysis of these plants, considering either the conventional systems or slight modifications. Many modifications have been suggested in the literature to improve the efficiency or some specific characteristics (e.g., power output, cost reduction and power plants efficiencies). Nevertheless, there is no cited work for simulation like this system for different site plant location under the Egypt climate. Therefore, the present work introduces a full modeling and simulation of solar plant has capacity 500 MW using the *MATLAB/SIMULINK* program for three locations in Egypt; Aswan, EL-Arish and Hurghada. This large capacity is selected due the high shortage in the electricity in Egypt and the government is ready to invest any large projects to cover this shortage. The objective of this model is to simulate and predict the hourly electricity output

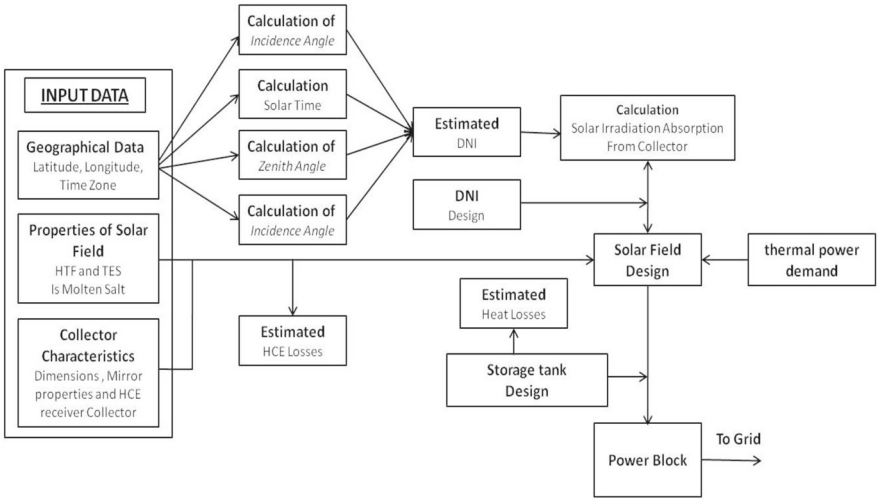

Fig. 2 Schematic representation of the performance model algorithm

during the day to obtain the effect of the storage tank on the plant performance. The thermal storage in the new design is working 16 h; The HTF solar salt (molten salt) which consists of 60% $NaNO_3$ and 40% KNO_3 was used in current work, due to its higher thermal stability (600 °C) and lower cost, especially, in these very large stations.

1.2 Work outlines

This work is comprised of six sections. The introduction section is explaining solar energy signification respect to Egypt and it also presents the introduction to solar parabolic trough technology followed by the literature review and work objectives. Section two introduces a mathematical model for CSPP (concentrated solar power plant) compounds. Methodology section is the third which gives brief about simulation tools and storage tank analysis followed by validation data in section four. The simulation results and discussion are given in section five. The paper has been closed by conclusions and suggestions for future work in section six.

2 Thermal and performance models

Figure 2 shows a schematic of performance model algorithm with the general structure of the information flow with the modeling. The left-hand side box of the figure summarizes the required inputs for simulation. These include geographical, properties of HTF and TES (thermal energy storage) data with addition collector type, these were required in different subsystems of the plant (solar field, thermal storage system, and power block).

2.1 Solar calculations and field model

Geographical data of the given site locations are used as input to the simulation performance model. Which include the latitude, l, longitude, ϕ, and the collector's orientation angle (zero rad for north or south orientation). The solar calculations and solar field model are explained in details as follows:

2.1.1 Direct normal irradiation (DNI)

The direct normal irradiation falling on horizontal surface is given by Jasmina and Amelija [34] as:

$$\mathrm{DNI} = \mathrm{I_{on}} \cos(\mathrm{z}) \tag{1}$$

The energy of extraterrestrial solar radiation that a unit of times falls at a right square meter can be calculated as follows, Jasmina and Amelija [34]:

$$I_{on} = \left[1 + 0.0333 \cos\left(\frac{360n}{365}\right)\right] I_{sc} \tag{2}$$

Zenith angle (z) is calculated as follows, Patnode [7]:

$$z = \cos^{-1}(\sin(l)\ \sin(\delta) + \cos(l)\ \sin(\delta)\cos(\mathrm{h})) \tag{3}$$

where l is the latitude angle (°), δ is the declination angle (°). The declination angle changes within a range of $-23.45° \leq \delta \leq 23.45°$ as rotation of the earth rotation around the sun. The declination angle is expressed by Patnode [7] as

$$\delta = 23.45 \sin\left(360\frac{284 + n}{365}\right) \tag{4}$$

As well, the hour angle is a result of the rotation of the earth on its axis (15° per hour) and it calculated by (Patnode [7]) as

$$h = (Solar\ time - 12) \cdot 15 \tag{5}$$

For adaptation, the relation between solar time and standard time is written as follows Patnode [7]:

$$Solar\ time = Standard\ time - DST + \frac{(L_{st} - L_{loc})}{15} + \frac{E}{60} \tag{6}$$

2.1.2 Angle of incidence (θ)

The angle of incidence on the collector can be calculated as a function in the declination angle, hour angle and zenith angle (Patnode [7]):

$$\cos\theta = \sqrt{\cos^2 z + \cos^2\delta\ \sin^2 h} \tag{7}$$

2.1.3 Solar irradiation absorption

Patnode [7] introduced an equation for calculating the absorbed solar radiation as:

$$q_{abs} = DNI \cdot \cos(\theta) \cdot IAM \cdot RShad \cdot ELoss \cdot \eta_f \cdot \eta_{HCE} \cdot FS_f \quad (8)$$

where q_{abs} is absorbed solar radiation by receiver tubes (W/m^2), Shad is row shadow factor (–), ELoss is losses performance factor (–), η_f is field efficiency (–), η_{HCE} is HCE efficiency (–), SF_f is fraction of the solar field that is operable and tracking the sun (–).

2.1.4 Incidence angle modifier (IAM)

Due to additional reflection and absorption by the glass envelope, the angle of incidence is correlated due to the losses in collectors. The equation for incidence angle modifier (IAM) for the collector is, (Isabel et al. [8]):

$$IAM = \cos(\theta) + C_1 \cdot \theta + C_2 \cdot \theta^2 \quad (9)$$

C_1 and C_2 are constants depending on the collector type; $C_1 = 0.000064$, $C_2 = -0.0000318$.

2.1.5 Row shadowing (RShad)

When the radiation incident on the collectors decreases, row shading decreases collector performance, Stuetzle [35]. The shading ratio is function in the solar zenith angle geometry and the incidence angle as well as the collectors' layout of the in a field:

$$RShad = \frac{W_{eff}}{W} = \frac{RS}{W} \cdot \frac{\sin(l)}{\cos(\theta)} \quad (10)$$

where, $RShad$ is row shadow factor (–), W_{eff} *is* effective width of mirror aperture (m), W is collector aperture width [5.75 (m) for LS-3]; RS is distance between two rows [18 (m)].

2.1.6 End losses (ELoss)

End loss occurs at the HCEs ends, the end loss is given by Lippke [11] as

$$ELoss = 1 - \frac{f \tan(\theta)}{L_{SCA}} \quad (11)$$

where f is focal length of the collectors [2.12 (m)], L_{SCA} is length of a single solar collector assembly (m).

2.1.7 Field efficiency and HCE efficiency

The field efficiency, η_f can be calculated taking in the account all the effects of surface and correction parameters for the collector assembly and mirror, Forristall [36] and Price [37]:

$$\eta_f = \sum_{i=1}^{Numcol} ColFr_i \cdot TrTwE_i \cdot GeAC_i \cdot MiRf_i \cdot MiCl_i \tag{12}$$

where $Numcol$: solar field collector types number, $ColFr$: solar field collector type fraction, $TrTwE$: collector tracking and twisting error, $GeAC$: collector mirrors geometric accuracy, $MiRf$: reflectivity of the mirrors, $MiCl$: cleanliness of the mirrors.

By the same idea, the HCE efficiency, η_{HCE} can be calculated as:

$$\eta_{HCE} = \sum_{i=1}^{NumHCE} HCEFrac_i \cdot HCEdust_i \cdot BelShad_i \cdot EnvTrans_i \cdot HCEabs_i \cdot HCEmisc_i \tag{13}$$

where $HCEFrac$: solar field HCE types number, $HCEFrac$: solar field HCE types friction, $HCEdust$: dust shading losses of HCE on the envelope, $BelShad$: ends shading losses of HCEs due to bellows, $EnvTrans$: glass envelope transmissivity, $HCEabs$: HCE selective coating absorptivity, $HCEmisc$: HCE miscellaneous losses factor.

Forristall [36] and Price [37] were discussed the optical parameter and correction values for solar field, they have been evaluated that the efficiency not exceed for solar field about 0.857 and HCE about 0.832.

The solar field is designed in this work with capacity 1500 MW_{th} (500 MW_{el} conversion efficiency of about third). The solar field consists of number of parallel connection loops of parabolic trough collectors. Every loop consists of some of solar collector assemblies (SCA) in one or more row in series connection. Every SCA consists of several solar collector elements (SCE), as illustrated in Fig. 3. To follow up the sun (from sunrise to sunset), the collectors tracking mechanism using single-axis can be used. The collector mirrors are used to reflect the solar energy and concentrate it onto the receiver tubes which heats up the HTF that circulate throughout the solar field.

2.1.8 Parabolic trough geometric

For the operation of a concentrator system power plant (CSPP) temperatures of around 550 °C are necessary. Concentrating collectors are used to obtain these high temperatures. The direct normal irradiation reaching the collector is concentrated on the absorber tube located in the focal point of the parabolic collector. Basic principle in the construction of the parabolic mirror is that, when parallel rays of sun lights from the sun parallel to the main axis are incident on a concave or parabolic shaped mirror. It

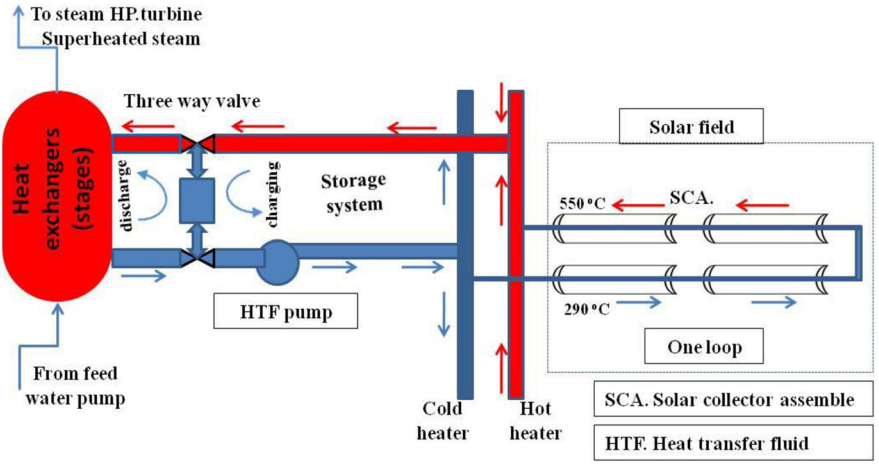

Fig. 3 Solar field components

comes together after reflection to appoint on the axis called principle focus. Therefore, the most important characteristic factor is the concentration ratio, CR. It is defined as the aperture in relation to the absorber area as in Horst [15].

$$CR = \frac{A_a}{A_{abs}} \tag{14}$$

$$CR = \frac{W}{\pi \cdot d_o} \tag{15}$$

where, A_a is aperture area (m^2); A_{abs} is absorber area (m^2); d_o is outer diameter of absorber tube (HCE) (m); W is aperture width for 5.75 (m).

2.1.9 Piping solar field

It is assumed that the multi "H" solar field layout as shown in Fig. 4, the features of this field as follows: (1) the solar field consists of 4 header-pair sections, where the power block is existed at the field center. Cold HTF is outflow from the cold header into solar fields from both header sides, flowing into rows of SCAs in series connection, and it is returned to the hot header throughout a similar set of SCAs arrangement. This configuration is known as a "loop". Accordingly, there are several and typical loops on both sides over the header length and the headers run east–west. (2) Every loop contains six SCAs (LS-3). HTF flows out from the cold header passing throughout three SCAs, reversing direction, and then it reverses its direction and returns to the hot header passing over the remaining three SCAs. (3) The flow pressure loss to the remotest loop is denoted by the pressure loss in the inner loops. (4) The cold header diameter is stepped down with increasing the distance from the power block to attain uniform fluid velocity and vice versa with hot header diameter.

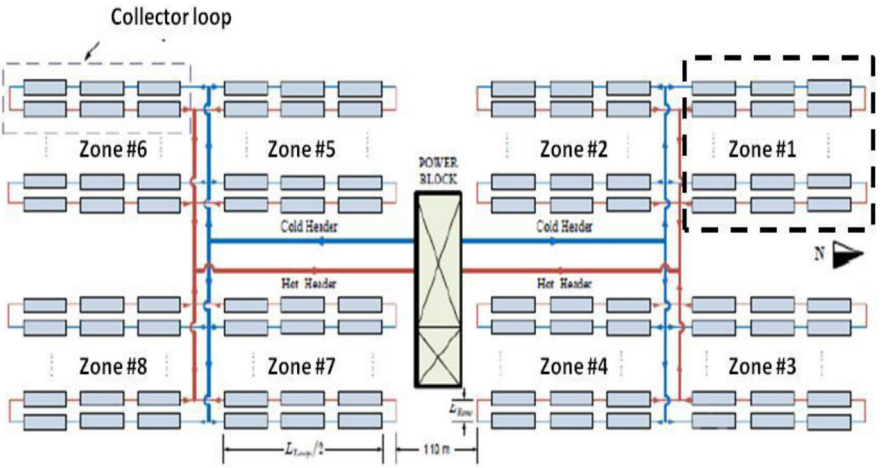

Fig. 4 Multi "H" solar field layout

2.1.10 Design optimization

In order to optimize the design, the initial design configuration and headers flow velocities are specified. In addition, the piping cost and pumping power are calculated which affect overall cost and performance. In this design variation is moderately flat for flow velocity, v ranges from 2 to 4 m/s with the smallest values at the flow end. To optimize (minimize) collector field piping arrangement, three issues should be considered: (1) pipes, insulation, and supports capital costs. (2) Thermal losses equivalent capital costs through the pipe insulation. (3) Electric energy equivalent capital cost for fluid circulation throughout the pipes.

2.1.11 Flow rate in the cold header

The flow rate M_{ms} (kg/s) in the east–west cold header for this design is calculated as follows:

$$M_{ms} = \frac{Q_{th}}{4\Delta h} = \frac{1500,000,000}{4\left(h_{@Toutf} - h_{@Tinf}\right)} \tag{16}$$

where Q_{th}: thermal rating of the collector field (J/s), Δh: enthalpy change between in and out solar field (J/kg).

2.1.12 Header pipe diameter

If flow rate is M_{ms} (kg/s), the header pipe inner diameter, D_{in} (m), can be calculated as follows:

$$D_{in} = \sqrt{\frac{4M_{ms}}{\pi * v * \rho(T)}} \tag{17}$$

Heat loss, Q from wall pipe surface expressed as:

$$Q = \alpha \cdot \pi D_i \left(T_f - T_a\right) \tag{18}$$

The heat transfer coefficient for HTF is calculated using correlations for forced convection heat transfer inside circular tube according to the basic convection heat transfer.

The total number of collector module as parabolic troughs, (N_{ctotal}) is function in the electrical power demand ($N_{cgenerating}$) and thermal energy storage ($N_{cstorage}$) to operate solar plant all times through day Forristall [6]. If q_{abs} is absorbed solar radiation, the total number of collector module can be calculated as follows:

$$N_{cgenerating} = \frac{Q_{th}}{q_{abs} \times L \times W} \tag{19}$$

$$P_{charging} = \frac{P_{th} \times time_{discharging}}{time_{charging}} \tag{20}$$

$$N_{cstorage} = \frac{P_{charging}}{q_{abs} \times L \times W} \tag{21}$$

$$N_{ctotal} = N_{cgenerating} + N_{cstorage} \tag{22}$$

2.1.13 Heat loss

The heat loss from HCE surface to surrounding can be calculated by:

$$q_{loss} = U_{loss} \cdot \pi d_o \cdot (T_w - T_a) \tag{23}$$

where q_{loss} is heat loss per collector length (W/m); U_{loss} is overall of heat loss (W/m^2 °C); d_o is outer diameter of absorber tube (HCE) (m); T_w is wall temperature of mirror collector (°C); T_a is ambient temperature of surrounding (°C), Forristall [6].

2.1.14 Thermal equilibrium for HCE

When sun radiation falls normal to the collector aperture area, most of this radiation are reflected to absorber tube via mirrors mounted on parabolic troughs then heats it to desired temperature (550 °C). The heat transfer balance occurs for HTF inside single HCE along one collector module (aperture area L × W).

The total thermal equilibrium equation for HCE a collector module can be written as Forristall [6]:

$$q_{abs} \times L \times W = Q_{LOSS} + M_{ms} \times C_P \left(T_{fout}(i) - T_{fin}(i)\right) \tag{24}$$

$$T_{fout}(i) = \frac{(q_{abs} \times L \times W) - (q_{loss} \times l)}{M_{ms} \times C_p} + T_{fin}(i) \tag{25}$$

$$No.\ of\ loops = \frac{N_{ctotal}}{N_{c/loop}} \tag{26}$$

The desired outlet temperature (550 °C) will be constant during the iterations to calculate the number of collector module even with variable mass flow rat of HTF.

2.1.15 HTF pump calculation

The power required for HTF of the variable speed pump is obtained by calculating the pressure drop (ΔP_{sf}) and total HTF mass flow rate, assuming all calculations under steady state condition. There are four types of the pressure drop in the system as follow: (1) pressure drop inside HCE pipe for the longest pass (the last interior point in HCE pipe, where HTF will arrive it), ΔP_{HCE}, for loop hot and cold heater with addition in and out solar field, $\Delta P_{in,out}$. (2) Pressure drop inside cold and hot heater, $\Delta P_{C,H}$. (3) Pressure drop for fitting pipe (expansion, valves of all kinds, elbows of all kinds, contraction…etc.), ΔP_{ff}. (4) Pressure drop inside shell-tube heat exchangers stages (HEX) ΔP_{HEX}.

It is required to calculate some parameters to complete the pressure drop calculations as follows: Reynolds number to determine flow type, Re, friction coefficient, f, and fluid properties function of HTF temperature Forristall [6].

$$Re = \frac{\rho(T) \times v \times D_i}{\mu(T)} \tag{27}$$

$$f = F\left(Re, \frac{\varepsilon}{D_i}\right) \tag{28}$$

Pressure drop inside any pipe is calculated by equation:

$$\Delta P = f \times \frac{1}{D_i} \times \frac{\rho(T)v^2}{2} \quad per\ unit\ length \tag{29}$$

Pressure drop fitting pipe is calculated by equation:

$$\Delta P_{ff} = K \cdot \frac{\rho(T)v^2}{2} \tag{30}$$

where K: fitting factor

$$Power_{pump} = \frac{\Delta P_{sf} \times Q_{ms}}{\eta_{pump}} \tag{31}$$

$$Q_{ms} = \frac{M_{ms,t}}{\rho(T)} \tag{32}$$

The pressure drop, ΔP_{sf}, in solar field according to the longest pass of HTF, is calculated as:

$$\Delta P_{sf} = \Delta P_{HCE} + \Delta P_{in.out} + \Delta P_C + \Delta P_H + \sum_{i=1}^{n} \Delta P_{i,i+1} @loop, C + \sum_{i=1}^{n} \Delta P_{i,i+1} @loop, H + \Delta P_{HEX} \quad (33)$$

2.2 Thermal storage tank calculation

Due to the low vapor pressure TES, the upright tanks with vertical field can be used. At atmospheric pressure, the big storage tanks are comparable to commercial ones. These tanks are constructed from carbon steel, using self-supporting roofs. The tanks wall and roof are insulated using mineral wool-batts and calcium silicate, respectively. The foundation insulation contents the following layers (from bottom to top): (1) concrete slab, (2) thermal foundation, (3) foam glass, (4) firebricks, (5) thin steel plate liner, and (6) sand. A perimeter ring from insulating firebricks is used to support the weight of the tank walls and roof, Herrmann et al. [10].

Generally, the energy that is involved in changing the temperature of the medium is called sensible heat, and it amounts simply to the product of the specific heat by the temperature change. It can be calculated by using these equations:

$$E_{stored} = \frac{\rho_{hms} \times V_{TES} \times c_{ph}(t) \times (T_{hot} - T_{cold})}{3.6 \times 10^6 \times t_{full\ load}} \quad (34)$$

$$E_{stored} = \frac{Gross\ power}{Desired\ efficicy} \times t_{full\ load} \quad (35)$$

$$D_{tank} = 2 \times \sqrt{\frac{V_{TES}}{h_{tank} \times \pi \times N_{pairs}}} \quad (36)$$

where h_{tank} is the tank height not exceeds 10 m; N_{pairs} is the number of tank pairs. The heat loss, q_{loss}, is calculated by:

$$q_{loss} = \left(\pi h_{tank} * D_{tank} + \pi * \left(\frac{D_{tank}}{2} \right)^2 \right) * C_{ph} N_{pairs} * (T - 20) \quad (37)$$

The minimum fluid volume, $V_{TES,min}$, is:

$$V_{TES,min} = V_{TES} * \frac{h_{min}}{h_{Tank}} \quad (38)$$

3 Simulation methodology

The "heart" of the CSPP is the power block. The thermal energy delivered either from storage or from the solar field transferred into electrical energy. The process has been described for how to harvest and transfer solar energy, as well as transport

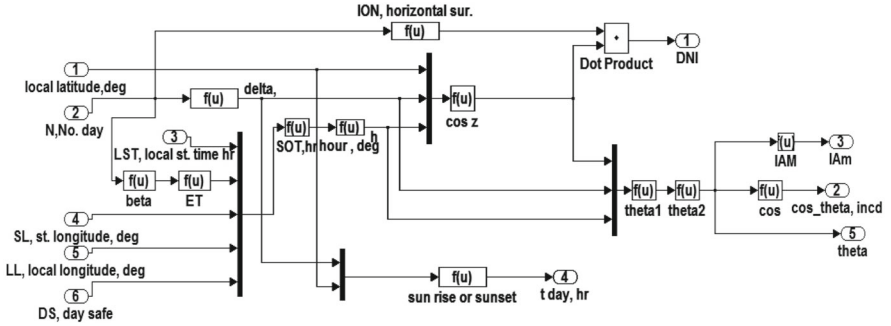

Fig. 5 Simulink model for the irradiation

Table 1 Inputs required to irradiation estimate

Inputs	Values
Location information, lat./long., °	(1) Aswan (Aswan) (23.97°N, 32.78°E) (2) Hurghada (Al Bahr al Ahmar) (27.15°N, 33.72°E) (3) EL-Arish (Shamal Sina) (31.08°N, 33.82°E)
Standard longitude, °	Egypt, 31.28°
Day number	21 June (no: 172) 21 December (no: 355)
Day time, h	24
Day safe, DS	0 or 1

and storage of thermal energy. For CSP plants, well-established techniques are used. These techniques are depending theoretically on the Clausius–Rankine cycle. The simulation algorithm and solar modeling have been created and simulated by *MATLAB/SIMULINK* program. The aim of this model is to design the stages of CSPP, prediction and analysis of the plant's electricity on a daily, monthly and yearly basis. That simulation is divided into three stages; solar field, storage system and power block.

3.1 Geographical data

In this section, a dynamic model is created to estimate all the details of the solar radiation falls on parabolic trough concentrators as shown in Fig. 5. Table 1 shows the input data that required for this model. The input data is inserted inside the model for three different locations in Egypt as mentioned before.

3.2 Absorption energy

The thermal energy absorption which required in the calculation of the HTF details is modeled. Input parabolic trough collector and HCE data are required to complete the simulation as well as some of calculated parameters from previous model as shown Fig. 6. Table 2 contains the dimension of collector and HCE data.

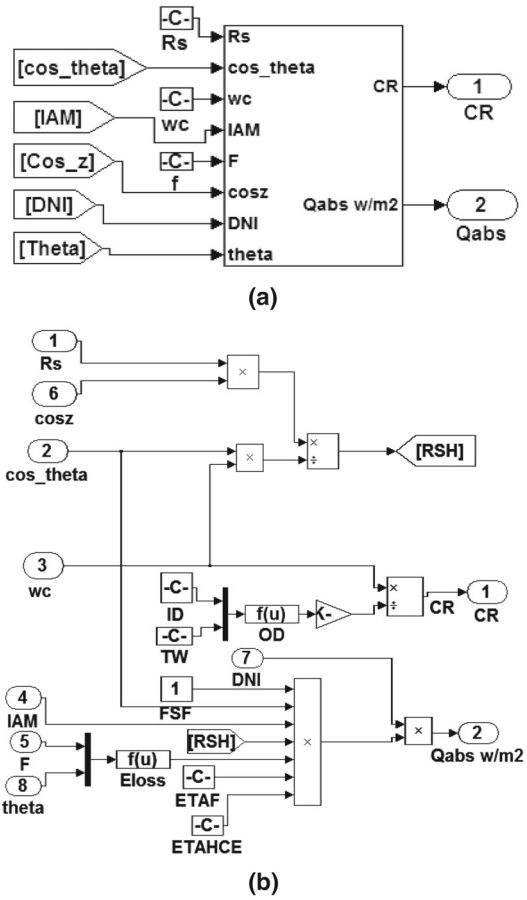

Fig. 6 Simulink model for the absorption energy, **a** block diagram input required, **b** details for block diagram

Table 2 Inputs required to calculate irradiation absorption

Inputs	Values
Module collector type Euro trough ET150	Wc = 5.75 m Lc = 12.5 m Rs = 18 m
HCE type	Schott PTR70 2008

3.3 Solar field

This section introduces a full design molding and performance calculations for solar field as shown in Fig. 7. The input data which required to this model are irradiation design, the demand power and thermal efficiency.

The outputs from this modeling solar design are concentration rate, total number of concentrator, number of loops, concentration per loop, total flow rate, minimum flow rate and maximum flow rate without storage. Table 3 shows the inputs required

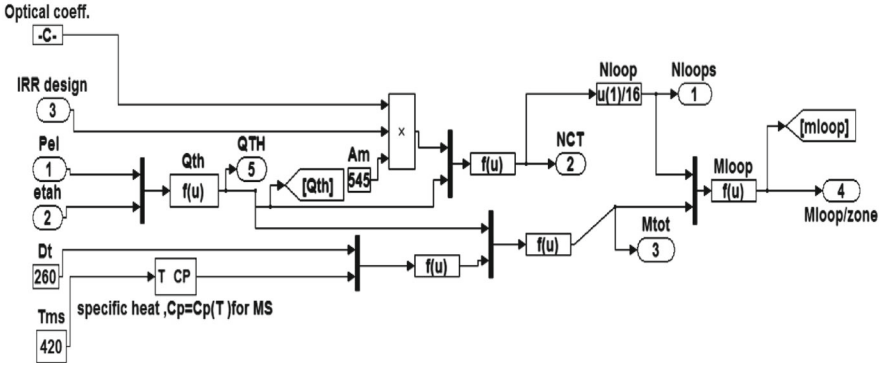

Fig. 7 Simulink model for solar field design

Table 3 inputs and output solar field design

state	Parameters	Values
Input design parameter	IRR design, W/m^2	600
	Gross power, MWe	500
	Thermal efficiency, %	0.333
	HTF inlet temperature, °C	290
	HTF outlet temperature, °C	550
	Solar multiple, (SM)	1
Output	Total concentration (module), Nct	41,472
	No. of loop, NLoop	864
	No. of collectors SCA's/loop	6
	No. of module/SCA	8
	No of module each loop Nm/loop	24
	No. of field section	8
	No. of loops/field	108
	Total volume of TES, m^3	109,994
	Full load hours of TES, h	16
	No. of parallel tank pairs	2
	The tank height, m	10
	The tank diameter, m	≈84
	flow rate/loop, kg/s	0.7
	Pressure drop each field, bar	25
	Minimum HTF pumped, kW/loop	1057.957
	Maximum HTF pumped, kW/loop	2026.504

and output values from this model. The total concentrators required depends on the intensity of DNI. Table 4 shows the total concentrators for three cities. It is clear that Aswan city has less number of concentrators, less number of loops and less number of solar fields.

Table 4 Total concentrators and number loops for three cities

City	Total concentrators	No. of loops	No. of solar field
Aswan	85,824	894	16.5
Al Bahr al Ahmar	133,440	1390	25.75
Shamal Sina	2,383,368	2483	46

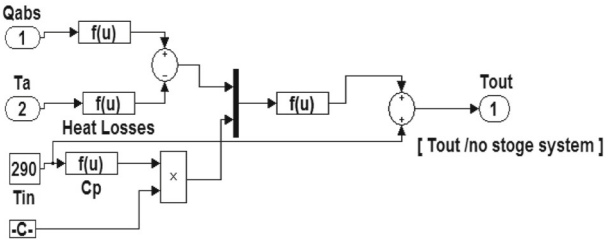

Fig. 8 Simulink HTF temperature without storage tank

3.4 Solar field outlet temperature

In this section, we can obtain the dynamic variation for HTF outlet temperature from solar field during throughout hourly day with and without storage tank. The dynamic absorption thermal energy and ambient temperature are calculated in this model by two ways:

- Without storage system (see Fig. 8).
- With storage system (see Fig. 9).

The main objective of the storage system is to compensate the absorbed solar thermal energy to produce desired temperature.

3.5 Power block simulation

The thermal energy delivered to the power block is the most significant input value for the performance calculation presented in this work. The theoretical basis for this simulation is the ideal Clausius–Rankine cycle. The efficiency increase is expected to be in the same range as the difference in efficiency between real and ideal Clausius–Rankine cycle. For the computation process, some design parameters are summarized in the Table 5. Figure 8 shows the calculated dynamic outlet temperature with add the inlet temperature along loop passing through assemble collectors' module.

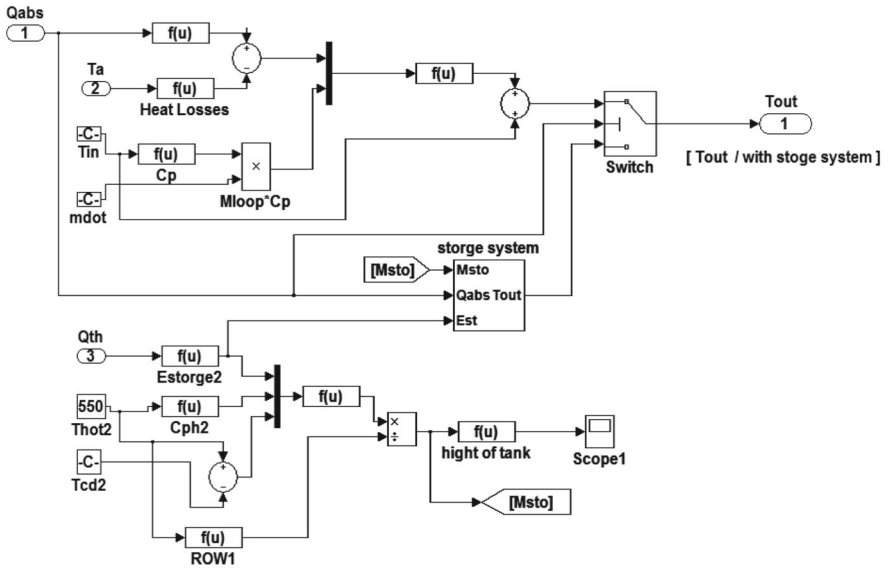

Fig. 9 Simulink HTF temperature with storage tank

Table 5 Design parameters required for simulation of the power block with a gross capacity of 500 MW_{el}. Source: The Southwestern Public Service Co.; Tolk Station

Parameters	Value
Pumps nominal efficiency, %	63
Steam turbine nominal efficiency, %	89
Generator nominal efficiency, %	98
Steam mass flow rate, kg/s	475.4
Temperature of steam, °C	537.8
Pressure of steam, bar	172.38
Reheat temperature, °C	537.8
Reheat pressure, bar	37.92
Nominal thermal load, MW_{th}	1500
Condenser pressure, cooling system Function (T condensation)	Wet and dry cooling

4 Model validation

Due unavailability information for solar plants with a large scale in the literature, so the available solar station is used as a model for validate current model. The Archimede plant [38] produces steam with gross capacity 5 MW_{el} from solar system (4.72 MW equivalents) and feeds a combined-cycle steam turbine rated at 130 MW. This parabolic trough system is the first station using molten salt as the heat transfer fluid with 8 h of thermal storage used through two tank direct system.

Table 6 Archimede plant characterizes

Geographical data	
Location information, °	Lat. 37.1342°N Long. 15.3834°E
Solar resource, (KWh/m^2/year)	1936
Solar field data	
Solar-field aperture area, m^2	$31{,}860 \approx 7\frac{2}{3}$ Feddan
# of solar collector assemblies (SCAs)	54
# of loops	9
# of SCAs per loop	6
SCA aperture area, m^2	590
SCA length, m	100
# of module per SCA	8
HCE type PTR70 wall thickness 3 mm	
# of HCE per SCAs	24
# of HCEs for solar field	1269
Power block	
Turbine capacity (gross), MW	5.0
Power cycle pressure, bar	93.83
Cooling method	Wet cooling

The heat collected in the solar field warms molten salt which goes between the cold tank which is at 290 °C and the hot tank which is at the desired temperature 550 °C, passing through the heat exchangers of the steam generators to produce the demand power. In the absence of solar energy, the thermal storage heating is used to avoid freezing inside HCE. The temperature is less than 220 °C and the rest of energy is used to cover the load. Table 6 shows the plant characteristics. The validation is presented for the solar field with storage system. In Table 7 the grey marked parts are the pre-entry parameters for the validation. According to the results in Table 7, it is clear that an acceptable agreement is obtained from the results of the simulation program in the present work and the actual results of the plant Arhimede. It also clear that the error rate does not exceed 0.05 respects to solar field performance calculation. In addition, for the thermal storage system calculation, the error rate does not exceed 0.01.

5 Results and discussions

As mentioned before, the present work introduces a deep description of the solar plant (CSP) in three different locations under the climate condition of Egypt. The hourly DNI and absorbed thermal energy for each location are presented in Fig. 10. Figure 10a, b shows a geographical study to determine the best solar properties in the three locations. Thus, it is clear that Aswan has the best solar characteristics, followed by Hurghada city and El-Arish city even if in summer (21 of June) or in winter (21 of

Table 7 validation data for solar field with storage system

Comparative items	Present simulation	Archimede plant
DNI design, W/m^2	650	650
HTF and TES properties (composition)	60% $NaNO_3$ 40% KNO_3	60% $NaNO_3$ 40% KNO_3
Thermal energy solar field, MW	13.16	12.5
Efficiency solar field, %	0.38	0.4
Storage hour, h	8	8
TES thermal capacity, MWh	105.26	100
Total mass of TES, tons	1605	1580
The volume of tank, m^3	880.475	866.760

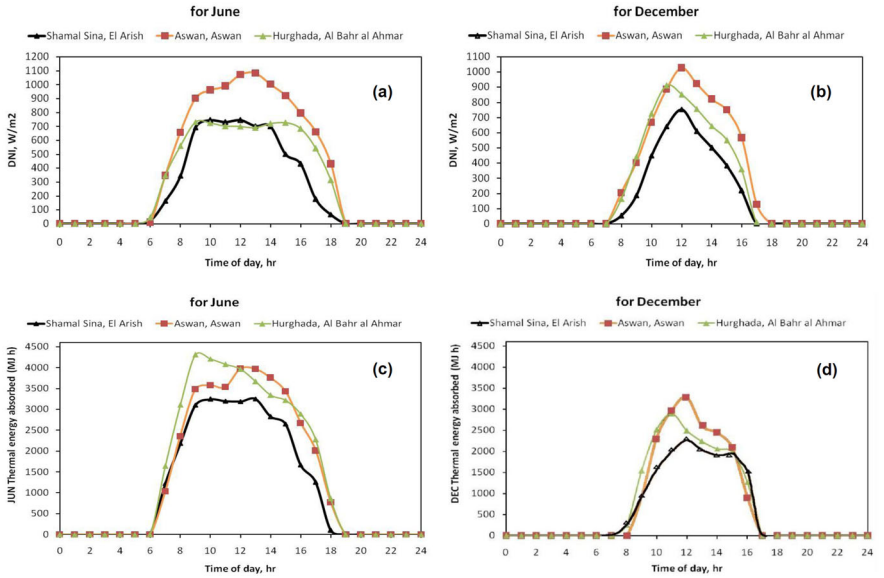

Fig. 10 DNI and thermal energy absorbed simulation for three cities in June and December

December). In spite of this, Fig. 10c, d shows that in the El-Arish city the absorbed thermal energy is higher than Aswan city during June and December. This is due to the number of concentrators in Aswan is less compared with the other two lactations. It is clear that, the solar intensity on day 21 of June (summer day) is stable along its day. Otherwise on day 21 December (winter day) is stable instance at certain time.

5.1 Aswan city

Figure 11a, b shows outlet temperature for hot header within solar field and dynamic change of volume for cold and hot tanks along 21 of June (summer day) and 21 of December (winter day). It is clear that for 21 of June day the temperature of hot header

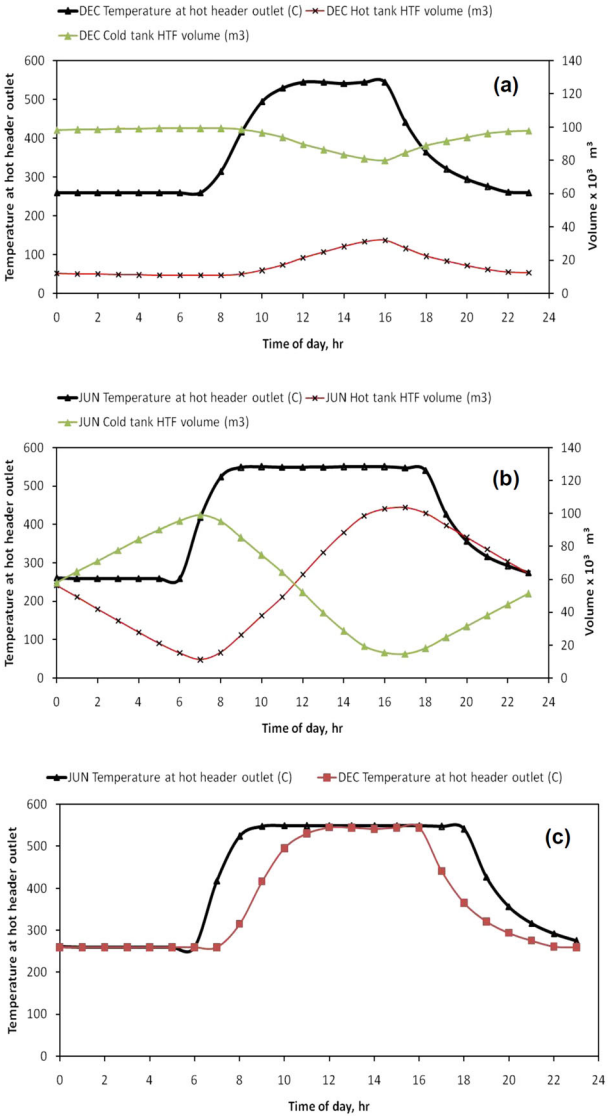

Fig. 11 Outlet temperature at hot header and discharge of hot and cold tanks for Aswan city: **a** June, **b** December, **c** comparison

takes short time to reach the desired temperature 550 °C. However, at 21 of December takes long time to reach the same desired temperature, around 2 h for summer day and about 4 h for winter day. With respect to charge and discharge for hot and cold tanks, Fig. 11a, b shows that the volume dynamic variation for summer and winter day. The results indicate that, the hot tank starts to charge at 7 am for summer day while at 9 am for winter day. The discharge of the hot tank starts at 5 pm for summer day and 4 pm at winter day and otherwise for cold tank. Moreover, it is noted that, the volume of TES inside tanks (hot and cold) is non-homogeneous variations during

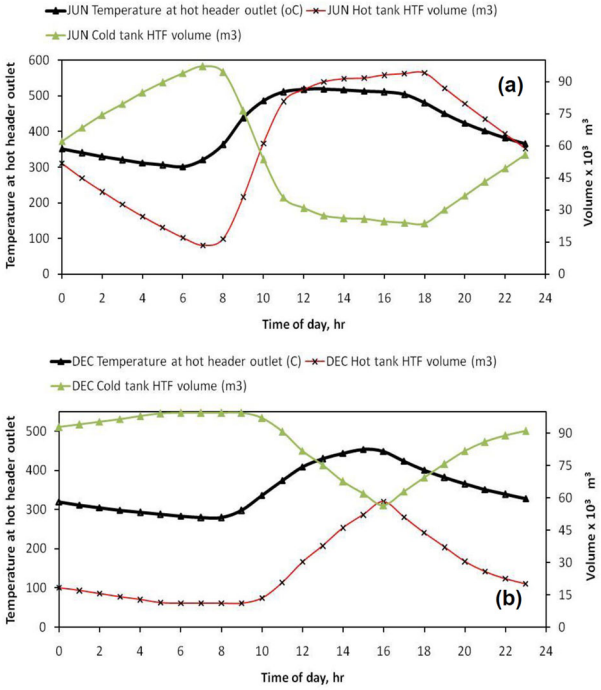

Fig. 12 Outlet temperature at hot header and discharge of hot and cold tanks for Al-Arish city: **a** June, **b** December

summer and winter day. Figure 11c shows a comparison between summer and winter days for outlet temperature for hot header. The main difference is the duration of the desired temperature 550 °C, in summer day the duration is longer than the winter day due to the difference in the solar day between the two seasons.

5.2 Al-Arish (Shamal-Sina) city

Figure 12a, b shows the outlet temperature dynamic variation for hot header within solar field and dynamic change of volume for cold and hot tanks along 21 of June (summer day) and 21 of December (winter day) for Al-Arish city (Shamal-Sina). It is clear that for 21 of June day the temperature of hot header takes long time to reach to the desired temperature 550 °C but instantaneously, it decreases to become 500 °C (not a designed point). Moreover, in winter day the outlet temperature did not reach to desired point, only 2 h for summer day and around four hours for winter day. Regarding the charging and discharging of the hot and cold tanks, Fig. 12a, b introduces the volume variation for summer and winter day. It is clear that, the hot tank was charging at 8 am in summer day, while, at 10 am in winter day. The discharge the hot tank starts at 6 pm for summer day, however, at 4 pm in winter day and otherwise for cold tank.

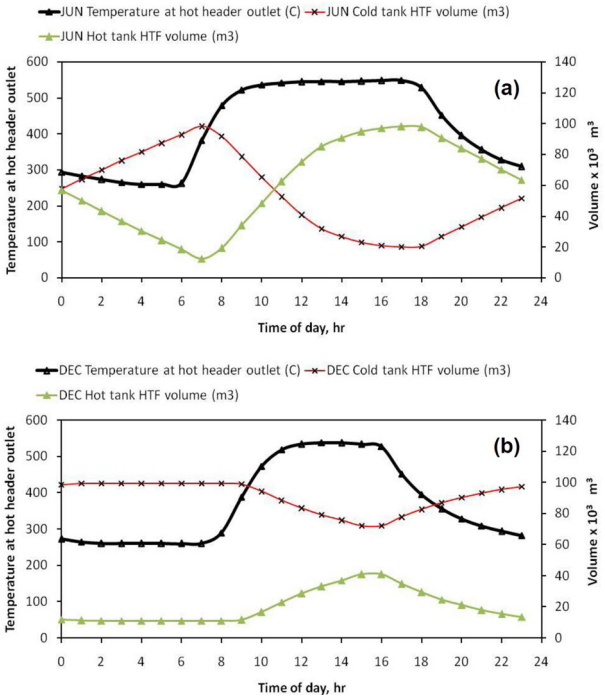

Fig. 13 Outlet temperature at hot header and discharge of hot and cold tanks for Hurghada city: **a** June, **b** December

5.3 Hurghada (Al Bahr al Ahmar) city

Outlet temperature dynamic variation for hot header is introduced within solar field and dynamic change of volume for cold and hot tanks along 21 of June (summer day) and 21 of December (winter day) for Al Bahr al Ahmar city (see Fig. 13a, b). In 21 of June day the temperature of hot header takes short time to reach to the desired temperature 550 °C, as for the 21 of December day takes longer time to reach to the same desired temperature; 3 h for summer day and about 4 h for winter day.

In addition, Fig. 13a, b also shows the volume dynamic variation for summer and winter days. It is clear that, the hot tank charging starts at 7 am for summer day while at 9 am for winter day. The discharge of the hot tank starts at 6 pm for summer day and 4 pm at winter day and otherwise for cold tank. Note that the volumes of TES inside tanks (hot and cold) have non-homogeneous variations during summer and winter days.

5.4 Plant site location comparisons

In this section, a comparison between Aswan, Al-Arish and Hurghada is introduced to select the best location to construct 500 MW solar power stations under the Egyptian climate. The selection criteria include three points of view in the comparison between

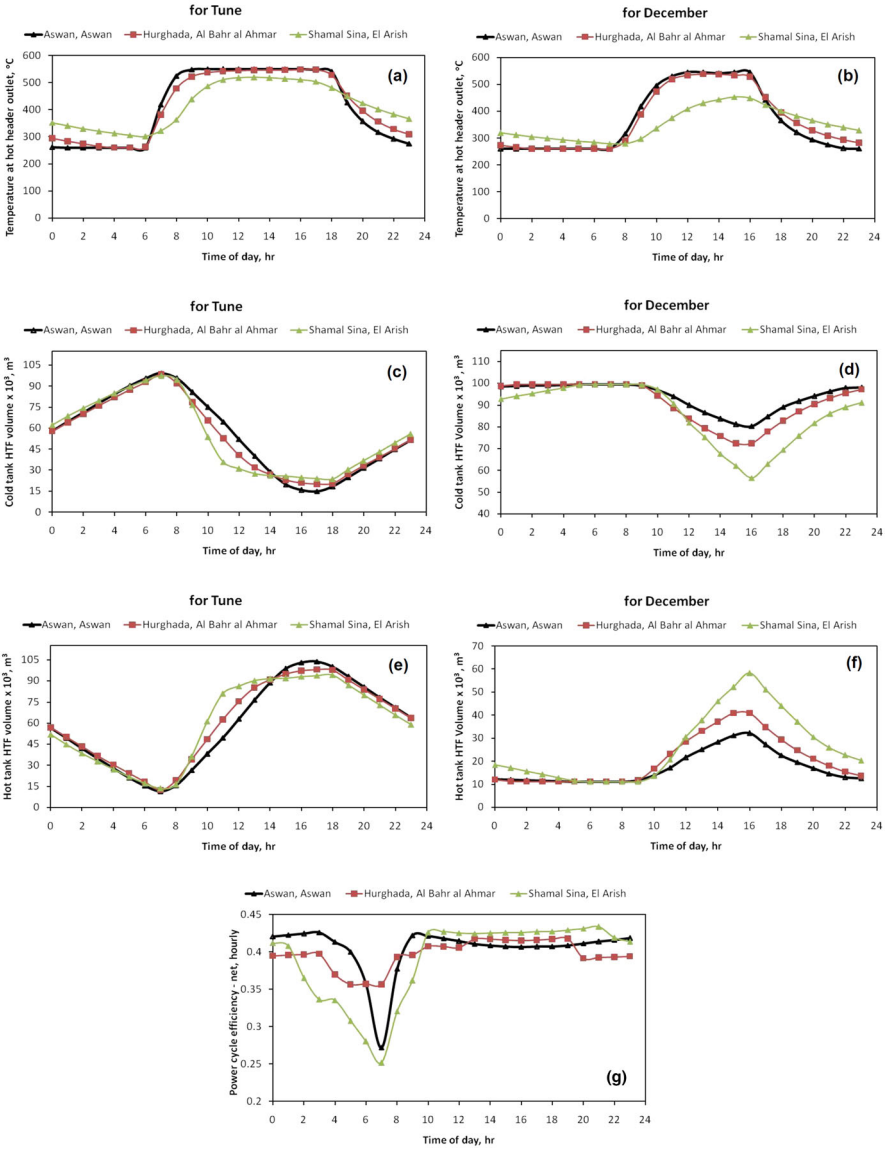

Fig. 14 Plant site location comparisons: **a**, **b** hot header outlet temperature, **c**, **d** cold tank HTF volume, **e**, **f** hot tank HTF volume, **g** power cycle efficiency

the different location; outlet temperature from hot header, volume (hot and cold) variations during charging and discharging, and cycle power efficiency. The three factors are investigated as follow, the outlet temperature for hot header (Fig. 14a, b), charge and discharge dynamic volumes of tank (Fig. 14c–f) and power cycle efficiency (Fig. 14g). According to these criteria, Aswan is the best location to constructed CSPP followed by Hurghada and the worst location is El Arish as shown in Fig. 14a–g).

Figure 14a, b indicates that the outlet temperature for Aswan as similar to Hurghada in summer and winter days. In Fig. 14c, d, the dynamic rate of the volume inside clod tank is the same for Aswan and Hurghada at summer day (21 of June) but at winter day the volume rated for Aswan is the higher. Otherwise at winter day for hot tank El Arish is the highest value for rated volume as shown in Fig. 14e, f.

Figure 14g shows that the power cycle efficiency for three locations. Aswan is the best location followed by Hurghada city. From these comparisons, Aswan is the optimum location to construct a 500 MW solar power plant under the Egyptian climate.

6 Conclusion

Some of interesting conclusions can be drawn from the simulation of parabolic trough concentrators using molten salt for HTF and TES molding as follows:

- The results revealed that there are total concentrator changes with location, the optimum location is Aswan, and number of modules is 85,824 to build 894 loops. While the worst location is Shamal Sina which needs 2,383,368 modules arranged in 2483 loops. However, Al-Bahr al-Ahmar needs 496 loops greater than Aswan.
- Total volume of storage tank is very huge, can be divided into ten pair tanks, each tank have height 10 m with 84 m diameter.
- The pressure drop along pipe equals 25 bars and mass flow rate is 0.7 kg/s for each loop.
- With respect to the charging and discharging time, in summer day the charging time starts at 7 am and discharge at 5 pm for Aswan. While winter day the charging time is starting at 9 am and discharge at 4 pm.
- Power cycle efficiency from 4 am to 7 am is the smallest efficiency in different locations due to the reduction of the HTF flow rate during this period.

References

1. Comsan, M.: Solar energy perspectives in Egypt. In: Proceeding of the 4th Environmental Physical Conference, Hurghada, Egypt (2010)
2. Lippke, F.: Simulation of the part-load behavior of a 30 MW SEGS plant. Prepared for Sandia National Laboratories, Albuquerque, NM, SAND95-1293 (1995)
3. KJC Operating Company (Power point Presentation).: Kramer SEGS facility solar electric generating systems III through VII. Last accessed 20 Oct 2004
4. Blair, N., Scott, A., Pitz-Paal, R., Schwarzboezl, P., Cable, R.: Concentrating "TRNSYS modeling of the SEGS VI parabolic trough solar electric generating system". In: Proceedings of Solar Forum 2001, Washington, D.C. (2001)
5. Stuetzle, A.: Automatic control of the 30 MWe SEGS VI parabolic trough plant. M.Sc, Department of Mechanical Engineering, University of Wisconsin-Madison (2002)
6. Forristall, R.: Heat transfer analysis and modeling of a parabolic trough solar receiver implemented in engineering equation solver. National Renewable Energy Laboratory, NREL/TP-550-34169 (2003)
7. Patnode, A.: Simulation and performance evaluation of parabolic trough solar power plant. M.Sc, University of Wisconsin-Madison (2006)
8. Isabel, L., Jose, L., Daniel, B.: Performance model for parabolic trough solar thermal power plants with thermal storage: comparison to operating plant data. Sol. Energy **85**, 2443–2460 (2011)

9. Fernandez, G., Zarza, E.: Parabolic-trough sola collectors and their applications. Renew. Sustain. Energy **14**, 1695–1721 (2010)
10. Hepbasli, A., Alsuhaibani, Z.: A key review on present status and Future directions of solar energy studies and applications in Saudi Arabia. Renew. Sustain. Energy Rev. **15**, 5021–5050 (2011)
11. Zhen, Y., Suresh, V.: Thermal analysis of solar thermal energy storage in a molten-salt themocline. Sol. Energy **48**, 974–985 (2010)
12. Bradshaw, R., Siegel, N.: Molten nitrate salt development for thermal energy storage in parabolic trough solar power systems. In: ASME Conference Proceeding, pp. 631–637 (2008)
13. Zhen, Y., Suresh, V.: Cyclic operation of molten-salt thermal energy storage in thermoclines for solar power plants. Appl. Energy **103**, 256–265 (2013)
14. Roberta, F., Antonio, C., Domenico, M.: Molten salt mixture properties in RELAP5 code for thermodynamics solar applications. Int. J. Therm. Sci. **47**, 1676–1687 (2008)
15. Horst, D.: Performance simulation for parabolic trough solar power plant and export scenario analysis for north Africa. M.Sc, Faculty of Engineering, Cairo University (2012)
16. Mohamed, M.H., William, G.E., Fatouh, M.: Solar energy utilization in water production from humid air. Sol. Energy **148**, 98–109 (2017)
17. William, G.E., Mohamed, M.H., Fatouh, M.: Desiccant system for water production from humid air using solar energy. Energy **90**, 1707–1720 (2015). https://doi.org/10.1016/j.energy.2015.06.125
18. Shaaban, S., Albatal, A., Mohamed, M.H.: Optimization of H-rotor Darrieus turbines' mutual interaction in staggered arrangements. Renew. Energy **125**, 87–99 (2018)
19. Ramadan, A., Yousef, K., Said, M., Mohamed, M.H.: Shape optimization and experimental validation of a drag vertical axis wind turbine. Energy **151**, 839–853 (2018)
20. Maizi, M., Mohamed, M.H., Dizene, R., Mihoubi, M.C.: Noise reduction of a horizontal wind turbine using different blade shapes. Renew. Energy **117**, 242–256 (2018)
21. Mohammadi, M., Lakestani, M., Mohamed, M.H.: Intelligent parameter optimization of Savonius rotor using artificial neural network and genetic algorithm. Energy **143**, 56–68 (2018)
22. Hashem, I., Mohamed, M.H.: Aerodynamic performance enhancements of H-rotor Darrieus wind turbine. Energy **142**, 531–545 (2018)
23. Hashem, I., Mohamed, M.H., Hafiz, A.A.: Aero-acoustics noise assessment for wind-lens turbine. Energy **118**, 345–368 (2017)
24. El-Baz, A.R., Youssef, K., Mohamed, M.H.: Performance assessment of an interactive three-rotor Savonius wind turbine. Renew. Energy **86**, 89–968 (2016)
25. Halder, P., Mohamed, M.H., Samad, A.: Wave energy conversion: design and shape optimization. Ocean Eng. **150**, 337–351 (2018)
26. Hashem, I., Abdel Hameed, H.S., Mohamed, M.H.: An axial turbine in an innovative oscillating water column (OWC) device for sea-wave energy conversion. Ocean Eng. **164**, 536–562 (2018)
27. Mohamed, M.H., Janiga, G., Thévenin, D.: Performance optimization of a modified Wells turbine using non-symmetric airfoil blades. ASME Turbo Expo 2008: Power for Land, Sea, and Air, pp. 2481–2488
28. Elattar, H.F., Fouda, A., Nada, S.A., Refaey, H.A., Al-Zahrani, A.: Thermal and hydraulic numerical study for a novel multi tubes in tube helically coiled heat exchangers: effects of operating/geometric parameters. Int. J. Therm. Sci. **128**, 70–83 (2018)
29. Elattar, H.F., Specht, E., Fouda, A., Bin-Mahfouz, A.S.: CFD modeling using PDF approach for investigating the flame length in rotary kilns. Heat Mass Transf. **52**, 2635–2648 (2016)
30. Elattar, H.F., Fouda, A., Nada, S.A.: Performance investigation of a novel solar hybrid air conditioning and humidification–dehumidification water desalination system. Desalination **382**, 28–42 (2016)
31. Elattar, H.F., Specht, E., Fouda, A., Bin-Mahfouz, A.S.: Study of parameters influencing fluid flow and wall hot spots in rotary kilns using CFD. Can. J. Chem. Eng. **94**, 355–367 (2016)
32. Nada, S.A., Fouda, A., Elattar, H.F.: Parametric study of flow field and mixing characteristics of outwardly injected jets into a crossflow in a cylindrical chamber. Int. J. Therm. Sci. **102**, 185–201 (2016)
33. Elattar, H.F., Fouda, A., BinMahfouz, A.S.: CFD modelling of flow and mixing characteristics for multiple rows jets injected radially into a non-reacting crossflow. J. Mech. Sci. Technol. **30**, 185–198 (2016)
34. Jasmina, R., Amelija, D.: Defining of the intensity of solar radiation on horizontal and oblique surface on earth. Work. Living Environ. Prot. **2**, 77–86 (2001)
35. Sargent and Lundy.: Assessment of parabolic trough and power tower solar technology costs and performance forecasts. NREL (2003)

36. Fernandez, D., Pitie, F., Caceres, G., Baeyens, J.: Thermal energy storage: how previous findings determine current research priorities. Energy **39**, 246–257 (2012)
37. Pranesh, K., Shreya, M., Rangan, B.: An analysis of costs of parabolic trough technology in India. Energy Policy **48**, 407–419 (2012)
38. https://www.nrel.gov/csp/solarpaces/project_detail.cfm/projectID=19. Last accessed 9 May 2018